Disinhibition mediated by reciprocal hypothalamic and raphé GABAergic projections promotes wakefulness

Mary Gazea[1,2,3*], Szabina Furdan[4*], Péter Sere[4,5], Lukas Oesch[1,2], Benedek Molnár[4,5], Giuseppe Di Giovanni[6,7], Susan M. Dymecki[8], Antoine R. Adamantidis[1,2¶] and Magor L. Lőrincz[4,5,6¶]

[1]Centre for Experimental Neurology, Department of Neurology, Inselspital University Hospital Bern, University of Bern, Bern, Switzerland

[2]Department of Biomedical Research (DBMR), Inselspital University Hospital Bern, University of Bern, Bern, Switzerland

[3]Present address: Concentris research management GmbH, 82256 Fürstenfeldbruck, Germany

[4]Department of Physiology, Anatomy, and Neuroscience, University of Szeged, Szeged, Hungary

[5]Department of Physiology, University of Szeged, Szeged, Hungary.

[6]Neuroscience Division, School of Bioscience, Cardiff University, Cardiff, UK

[7]Department of Physiology and Biochemistry, University of Malta, Malta

[8]Department of Genetics, Harvard Medical School, Boston, MA, USA.

[*¶]equal contribution

Correspondence should be addressed to Magor L. Lőrincz: mlorincz@gmail.com or Antoine R. Adamantidis: antoine.adamantidis@dbmr.unibe.ch

Keywords: arousal, brain states, neuromodulation, inhibition, GABA, optogenetics, disinhibition

ABSTRACT

The lateral hypothalamus (LH), together with multiple neuromodulatory systems of the brain, such as the dorsal raphé nucleus (DR), is implicated in arousal, yet interactions between these systems are just beginning to be explored. Using a combination of viral tracing, circuit mapping, electrophysiological recordings from identified neurons and combinatorial optogenetics, we show that GABAergic neurons in the LH selectively inhibit GABAergic neurons in the DR resulting in disinhibition of a substantial fraction of its neurons that ultimately promotes arousal. These DR GABAergic neurons are wake active and project to multiple brain areas involved in the control of arousal including the LH, where their specific activation potently influences local network activity leading to arousal from sleep. Our results show how mutual inhibitory projections between the LH and the DR promote wakefulness through disinhibitory mechanisms and suggest a complex arousal control by intimate interactions between long-range connections and local circuit dynamics.

Introduction

State-dependent neuronal activity across sleep-wake states, as revealed by cortical EEG, is determined by the activity of thalamo-cortical networks~~,~~ the septo-hippocampal formation and neuromodulatory systems (Saper et al., 2010; Weber and Dan, 2016). Brain states are greatly influenced by the diffuse neuromodulatory systems located in the brainstem (Constantinople and Bruno, 2011; Eggermann et al., 2014; Reimer et al., 2016), the basal forebrain (Jones, 2020) and the lateral hypothalamus (LH) (Bonnavion et al., 2016; Herrera et al., 2016). The LH encompasses distinct cell populations implicated in the modulation of arousal (Saper et al., 2001) and control of energy intake (Bernardis and Bellinger, 1996). Hypocretins/orexins and MCH neurons of the LH control wakefulness (Adamantidis et al., 2007; Carter et al., 2009) and REM sleep (Jego et al., 2013; Konadhode et al., 2013; Tsunematsu et al., 2014), respectively, through direct modulation of noradrenergic or histaminergic systems (Carter et al., 2010; Jego et al., 2013).Yet, whether and how the LH can also impact on the activity of other brainstem neuromodulatory circuits remains unclear. Of these, the dorsal raphé (DR) serotonergic system is an appealing candidate for influencing brain states based on various internal functions since it rapidly (~1 s) influences sensory (Kapoor et al., 2016; Lottem et al., 2016), motor (Liu et al., 2014; Correia et al., 2017; Seo et al., 2019) and cognitive (Miyazaki et al., 2011; Liu et al., 2014; Cohen et al., 2015; Fonseca et al., 2015) functions. Importantly, the DR and its major neuromodulator serotonin (5-hydroxytryptamine, 5-HT) has been involved in the regulation of various (patho)physiological functions including depression (Lowry et al., 2008).

Controversies about the role of the 5-HT system in sleep-wake states have remained throughout the years (Oikonomou et al., 2019). Electrophysiological studies showed that putative 5-HT neurons in the DR are highly active during wakefulness, decrease firing during non-rapid eye movement (NREM) sleep, and cease firing during REM sleep (McGinty and Harper, 1976;

Trulson and Jacobs, 1979; Sakai, 2011), although heterogeneity of firing amongst DR neurons has been reported (Urbain et al., 2006). Consistent with these recordings, brain 5-HT levels are highest during wake, lower during NREM sleep, and lowest during REM (Portas et al., 2000). Furthermore, pharmacological studies provided evidence for a wake-promoting function of 5-HT (Monti, 2011). Blockade of 5-HT2 receptors promotes sleep in humans (Idzikowski et al., 1986) and rats (Dugovic and Wauquier, 1987), but increases wakefulness in cats (Sommerfelt and Ursin, 1993). By contrast, 5-HT was originally identified as a sleep-promoting neuromodulator since depletion of serotonin (Torda, 1967; Koella, 1968; Mouret et al., 1968), ablation (Jouvet, 1968, 1972) or cooling (Cespuglio et al., 1976) of the raphe area produced transient insomnia. The sleep-promoting effect of 5-HT was partly confirmed in experimental studies where 5-HT1AR agonists decreased wakefulness when administered locally, but increased wakefulness when administered systemically (Fiske, 2008) and 5-HT2A KO mice showed reduced sleep, although systemic treatment with a 5-HT2A receptor antagonist increases sleep (Popa et al., 2005).

Interestingly, optogenetic stimulation of DR 5-HT neurons either promotes arousal and decreases sleep (Ito et al., 2013) or induces sleep (Oikonomou et al., 2019) depending on the pattern of stimulation. Accordingly, optogenetic inhibition of 5-HT DR neurons using ePet-cre mice blocked arousal in response to high levels of CO2 (Smith et al., 2018). Yet, embryonic ablation of TPH2 does not alter total sleep levels in mice (Solarewicz et al., 2015), while genetic ablation of TPH2 in the raphe nuclei (groups B5–B9) or Pet -positive neurons (using ePet-cre mice) of adult mice caused hyperactivity and eliminate siestas (Whitney et al., 2016) and a reduction only in REM sleep (Iwasaki et al., 2018), respectively.

These contrasting findings likely result from the heterogenous cell types present in the dorsal and median raphe nuclei, their diffuse pattern of axon projections, their heterogeneous firing

91 patterns across the sleep-wake cycle, and the multiple serotonin receptors expressed in the
92 central nervous system (Pytliak et al., 2011; Sakai, 2011). Indeed, the largest fraction of DR
93 neurons are non-serotonergic (Descarries et al., 1982), express the VGAT marker (Allers and
94 Sharp, 2003) and project to various forebrain targets including the LH (Bang and Commons,
95 2012).
96 Using a combination of combinatorial optogenetics, *in vivo* and *in vitro* electrophysiological
97 recordings from identified neurons, we show that GABAergic neurons in the LH selectively
98 inhibit DR GABAergic neurons resulting in disinhibition of a substantial part of DR neurons
99 that ultimately promotes wakefulness. We found that DR GABA neurons are highly active
100 during wakefulness compared to NREM and REM sleep, project to multiple brain areas
101 involved in the control of arousal including the LH, where their specific activation potently
102 influences local network activity leading to wakefulness. These results highlight the importance
103 of rapid hypothalamic control of a major neuromodulatory system and emphasize the
104 importance of long range subcortical inputs in controlling neuromodulatory systems affecting
105 brain states.

106 **RESULTS**

107

108 **LH GABAergic projections to the DR promote wakefulness**

109 A subpopulation of LH VGAT (vesicular GABA and glycine transporter) neurons causally
110 promotes arousal from NREM sleep (Herrera et al., 2016; Venner et al., 2016). Here, we tested
111 the role of LH VGAT projections to the DR in the control of sleep-wake behaviour. To deliver
112 opsins to LH VGAT neurons, Vgat-Cre mice were stereotactically injected with AAV2-EF1a-
113 DIO-eYFP (control) or AAV2-EF1a-DIO-hChR2(H134R)-eYFP) (ChR2-EYFP) in the LH for
114 *in vivo* optogenetic activation experiments (see methods; Fig. 1A and B). Mice were then
115 implanted with EEG/EMG electrodes for the recording and quantification of sleep-wake states
116 together with an optic fibre above the DR (see methods; Fig. 1C and D). State-specific
117 optogenetic activation of LH VGAT fibres in the DR was triggered manually after at least 10
118 seconds in stable NREM or REM sleep. Blue light (473 nm) was delivered to the DR at 5Hz or
119 20Hz (5ms pulses) in both control (eYFP) and ChR2-expressing animals continuously until a
120 state transition occurred (Fig. 1E). Interestingly, optogenetic activation of LH VGAT
121 projections to the DR during NREM sleep led to a rapid arousal at both 5 and 20 Hz within <
122 7s (Fig. 1F, $P < 0.0001$, three-way ANOVA), whereas optical activation of these fibres failed
123 to significantly change REM sleep duration (Fig. 1G). These results extend previous
124 mechanisms for LH VGAT induced arousal to DR neurons in the brainstem.

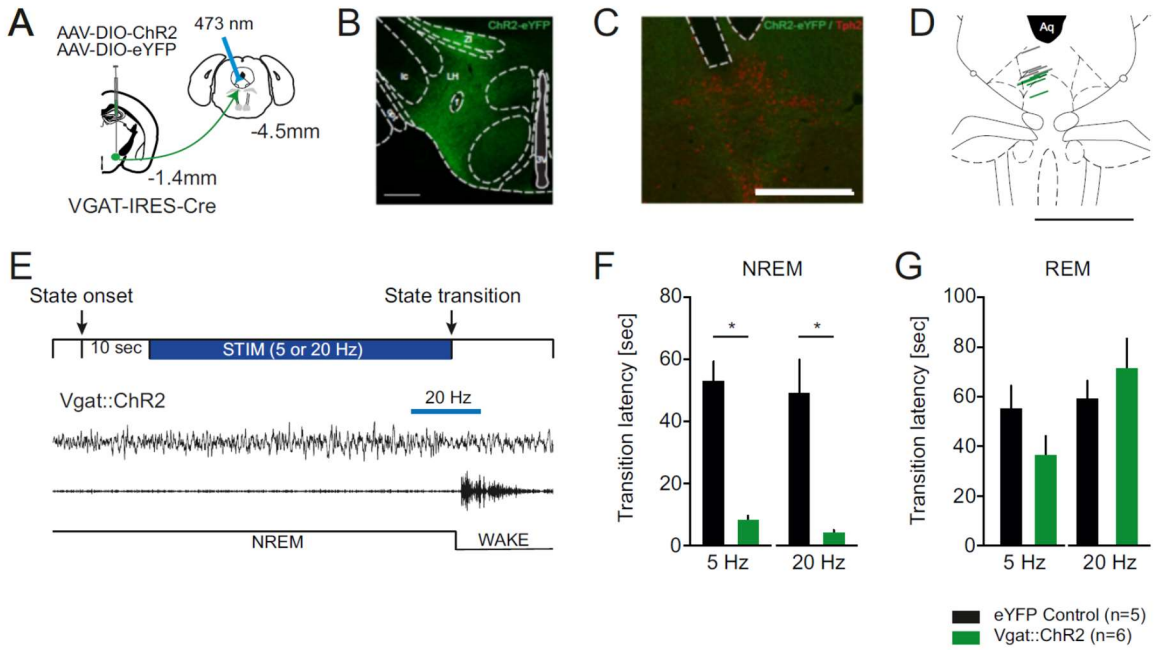

Figure 1. Stimulation of LH GABAergic fibers in the DR promotes wakefulness. (A) Schematics of the experimental design: AAV-DIO-ChR2-eYFP or AAV-DIO-eYFP was injected in the LH of Vgat-cre mice. Following 4 weeks of expression LH GABAergic fibers were photostimulated in the DR with simultaneous polysomnographic recordings for sleep stage scoring. (B) Example ChR2-eYFP expression in the LH. Fluorescent image overlaid on the stereotaxic atlas (Paxinos, AP: 4.45). (C) Location of the optical fiber in the DR used for photostimulation. Merged fluorescent image showing LH GABAergic fibers expressing ChR2-eYFP (green) and TPH immunhistochemistry (red) to indicate the location of TPH synthetizing serotonergic neurons within the DR. (D) location of all implanted optical fibers in 11 mice. Green lines: Vgat::ChR2-expressing mice (n=6), gray lines: eYFP controls (n=5), Aq: aqueduct). (E) (Top) Schematic experimental timeline for sleep-stage specific photostimulation. (Bottom) Representative EEG/EMG traces illustrate behavioural response to optogenetic stimulation. Note the rapid EEG desynchronization and EMG activation upon photostimulation indicating a NREM-to-Wake transition. (F) Latency of NREM to wake transition caused by the photostimulation of LH GABAergic axons in the DR. (G) Latency of

141 REM to wake transition caused by the photostimulation of LH GABAergic axons in the DR. *
142 $P < 0.05$.

143

144 **LH to DR GABAergic projections can rapidly suppress the activity of DR GABAergic**
145 **neurons**

146 To test the functional role of GABAergic LH to DR projections, we recorded extracellular
147 single unit activity from morphologically and neurochemically identified neurons in the DR of
148 anesthetized Vgat-cre mice transduced with AAV-flex-ChR2 in the LH while photo-stimulating
149 ChR2 expressing LH axons in the DR (5 light pulses of 10 ms at 20 Hz, 5 mW; Fig. 2A).

150 When comparing the activity of DR neurons upon LH GABAergic axonal photo-stimulation,
151 we found a rapid suppression (peak suppression: 42.37±5.94%, Fig 2B) of neuronal activity
152 (baseline firing: 7.72±6.43 Hz, baseline firing rate after photostimulation: 5.37±6.77 Hz, n=25,
153 $p < 0.001$, Wilcoxon's signed rank test, Fig 2D and E). We identified the morphology of 8
154 neurons and the neurochemical identity of 3 of these neurons (38%) was confirmed to be
155 GABAergic based on positive immunohistochemical reaction to Vgat (Fig 2C). These results
156 show that LH GABAergic neurons exert a potent inhibitory action onto identified and putative
157 DR GABAergic neurons.

158 We next explored the effect of stimulating LH GABAergic fibers in the DR in awake, head-
159 restrained animals while recording the activity of multiple single units in the DR (see Methods).
160 Comparison of the activity of DR neurons recorded in the presence and absence of LH
161 GABAergic axonal photostimulation (5 light flashes of 10 ms at 20 Hz, 5 mW) further
162 confirmed the strong inhibitory effect onto a subset of DR neurons (2/12, 17%), while the
163 activity of the remaining neurons was increased (10/12, 83%). The overall activity of DR
164 neurons was slowly (~200 ms), but persistently (~1 sec) increased (baseline firing: 7.67±6.87

Hz, baseline firing after photostimulation: 10.98±8.920 Hz, n=12, $p < 0.001$, Wilcoxon's signed rank test, Fig 2F and G).

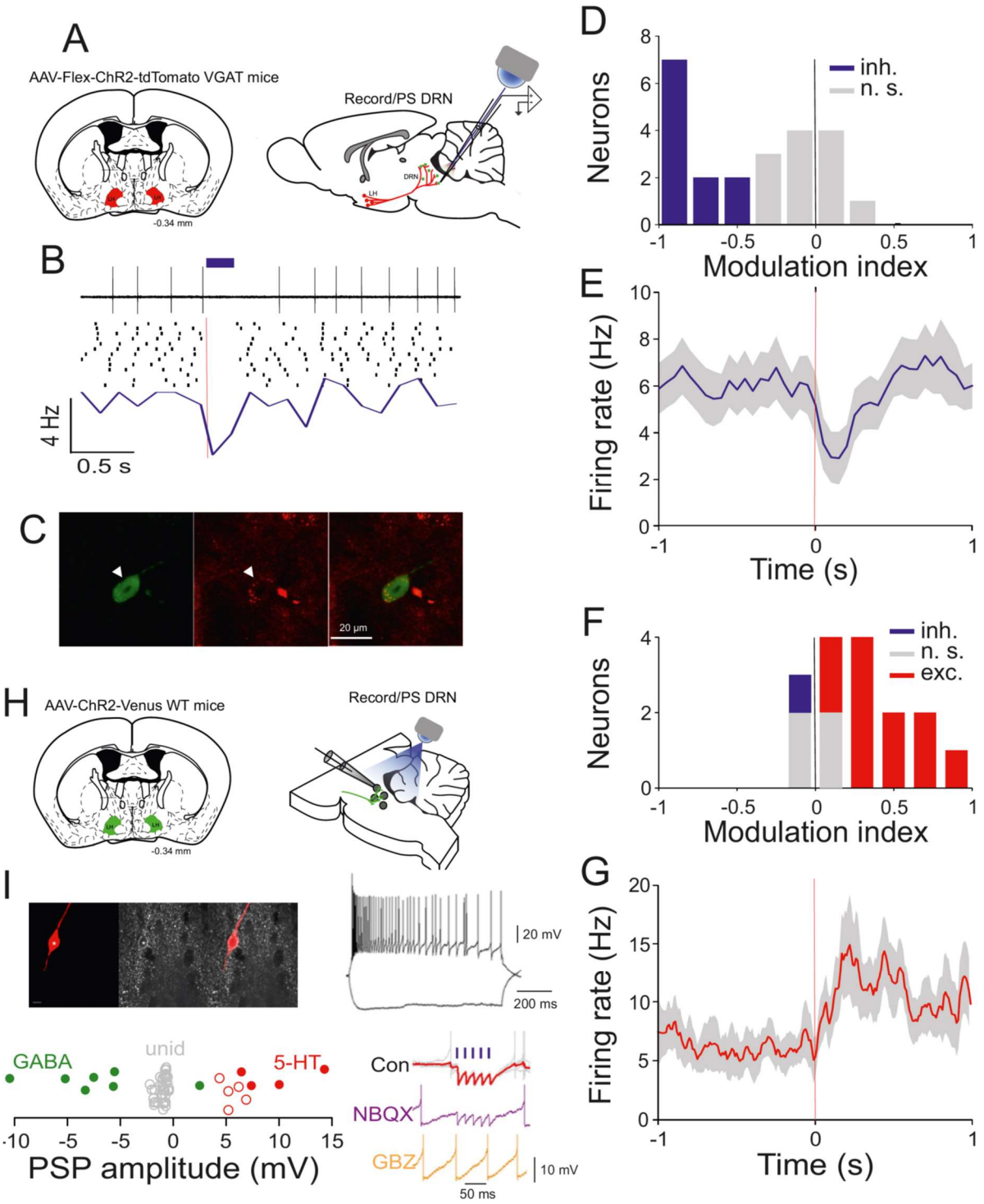

Figure 2. LH GABAergic projections control the activity of DR neurons. (A) Schematics of the experimental design: AAV-Flex-ChR2 injection in the LH of VGAT mice leads to prominent ChR2 expression in DR projecting axons. 4 weeks after the infection local axons of LH GABAergic neurons are photostimulated in the DR with simultaneous single unit juxtacellular recoding/labeling. (B) Example of spontaneous activity of a DR GABAergic neuron and its response to local photostimulation of LH GABAergic axons. (Top) Single-trial raw data aligned on photostimulation onset (blue horizontal bar, 5 mW, 10 ms pulses at 50 Hz). Middle, Raster plot in which each tic is a single-unit spike and each row represents a single trial. Red line: photostimulation onset. (Bottom) PSTH of the unit shown above. (C) Fluorescent pictures showing the neuron recorded in (B) filled with Neurobiotin using the juxtacellular filling technique (see Methods). Left: streptavidin, middle: VGAT immunostaining, right: merged picture. (D) Modulation index of all recorded neurons under anaesthesia. (E) Grand average PSTH of all neurons recorded neurons under anaesthesia. (F) Modulation index of all recorded neurons in awake animals (inh: inhibited, n.s.: not signifficant, exc: excited). (G) Grand average PSTH of all neurons recorded neurons under anaesthesia. (H) Schematics of the experimental design: AAV-ChR2-Venus injection in the LH of WT mice leads to prominent ChR2 expression in DR projecting axons. After 4 weeks after the infection local axons of LH GABAergic neurons are photostimulated in the DR with simultaneous whole-cell patch clamp recordings in identified DR neurons. (I) (Top, left) Fluorescent images (Streptavidin, GABA immunostaining, merged) of a DR GABAergic neuron responding to LH axonal photostimulation. (Top, right) Membrane potential responses to hyperpolarizing and depolarizing current steps shows fast action potential output with moderate frequency adaptation. (Bottom, right) The photostimulation of LH axons leads to monosynaptic IPSPs that are resistant to iGluR blockade (NBQX), but blocked by SR-95531 (GBZ, gabazine). (Bottom, left) Distribution of PSP amplitudes in all the neurons recorded (n). Filled circles indicate

194 identified GABA (green) or 5-HT (red) neurons, open circles putative GABAergic (green) or
195 5-HT (red) neurons, unid: unidentified neurons.

196

197 **DR neurons receive monosynaptic inputs from LH GABAergic cells**

198 In order to determine the downstream circuitries mediating this rapid arousal response, we
199 mapped LH GABA efferents utilizing ChR2-assisted circuit mapping after stereotactic injection
200 of AAV-ChR2-td-tomato into the LH of VGAT-cre mice. We previously found that
201 LH_{GABA} neurons send long-range projections to various brainstem nuclei, including the DR
202 (Herrera et al., 2016).

203 Next, we used optogenetics to functionally characterize this LH-DR circuit. We found that
204 photostimulation of AAV-syn-ChR2-Venus (Petreanu et al 2009) expressing LH terminals in
205 the DR evoked inhibitory postsynaptic potentials (IPSPs, -7.9±1.03 mV peak amplitude with a
206 10,91±2,41 ms decay time) in 8 DR cells (20%) recorded (Fig. 2I), while EPSPs of 7.58±0.9
207 mV peak amplitude with a 11,07±2,46 ms decay time were recorded in 10 (15%) DR cells (Fig.
208 2I). No detectable PSPs could be recorded in the remaining population, n=34, 65%). The IPSPs
209 could be abolished by SR95531 (i.e. gabazine, n= 5 out of 5 cells, 100%, Fig 2I) but not NBQX
210 (n=0/5, 0%, Fig 2I), suggesting that these are monosynaptic pathways implicating GABAa
211 receptors. Note that this result was further confirmed by the recording of similar IPSPs upon
212 photostimulation of LH axon terminals in the presence of TTX and 4-AP (mean IPSP
213 amplitude: control: 4.7±0.9 mV, TTX/TEA: 3.15±0.8 mV, n=5 neurons, data not shown). When
214 neurons were held at membrane potentials close to action potential initiation threshold,
215 photostimulation of LH axons also led to a prominent suppression of firing (12.66±6.65 Hz vs.
216 0 Hz, MI -1.0, n=3 neurons) due to the presence of large amplitude IPSPs (Fig 2I). This

217 suppression of firing was fully abolished when IPSPs were blocked by gabazine (n=3/3, Fig
218 2I).

219 The EPSPs were completely blocked by the AMPA/KA receptor blocker NBQX (n=5 out of 5
220 cells, Suppl Fig 2), but persisted in the presence of TTX and 4-AP (mean EPSP amplitude:
221 control: 5.68±0.49 mV, TTX/4-AP: 2.88±0.42 mV, n=5 neurons, data not shown). When
222 scrutinizing the neurochemical identity of the neurons recorded following either post-hoc
223 immunohistochemistry (against GABA or 5-HT) or when recording fluorescent GABAergic
224 neurons in G42 mice (JAX stock #007677) (Chattopadhyaya et al., 2004) we found that the
225 PSPs were EPSPs in all serotonergic neurons, but IPSPs in most GABAergic neurons. These
226 results show that the LH to DR projections are functional, can be either inhibitory or excitatory,
227 and show cell-type specific preferences within the GABAergic and serotoninergic neuronal
228 populations of the DR.

229

230 **The activity of identified DR GABA neurons is brain state dependent**

231 To target GABAergic neurons in the DR, we made use of the intersectional virus approach
232 (Fenno et al., 2014), in which Pet1^{Flpe} - Vgat^{Cre} double transgenic mice (Jensen et al., 2008;
233 Vong et al., 2011) were injected with an adeno-associated virus (AAVdjd) that was both Cre-
234 and Flp-dependent (see methods; Fig. 4A). We used this approach to exclude the possibility
235 that GABAergic markers (Vgat) are co-expressed with serotonergic neurons(Huang et al., 2019;
236 Ren et al., 2019; Okaty et al., 2020) by targeting distinct subpopulations of the DR with ChR2-
237 eYFP that were either Pet1-OFF/Vgat-ON or Pet1-ON/Vgat-ON. The Pet1-OFF/Vgat-ON
238 GFP-positive neurons co-localized with Vgat neurons that were co-transfected with a Cre-
239 dependent mCherry virus (Fig. 3B).

240 To investigate whether the activity of GABA neurons in the DR is modulated across sleep-wake
241 states, we performed opto-tag unit recording of putative DR Pet1-OFF/Vgat-ON neurons while
242 simultaneously conducting EEG and EMG recordings in freely moving Pet1^{Flpe}-Vgat^{Cre} mice
243 (see methods; Fig. 3C). These neurons were identified by their immediate increase in spiking
244 in response to short blue light pulses (10 times 5ms pulses, every 30 seconds) delivered to the
245 DR via an optic fiber. A total of 9 optogenetically identified Pet1-OFF/Vgat-ON neurons (9 out
246 of 66 cells from 4 animals; Fig. 3D and E) were recorded during wakefulness (Fig. 4F). The
247 activity of Pet1-OFF/Vgat-ON neurons was modulated across sleep-wake states (Fig. 3F-H,
248 NREM vs Wake/REM: $P < 0.05$, Friedman non-parametric test). Indeed, their firing activity
249 increased significantly upon arousal as compared to the 5 seconds before the transition occurred
250 (, i.e., when the muscle tone was still low; Fig. 3F,G and I; NREM-to-wake $P < 0.01$; REM-to-
251 wake $P < 0.05$, paired t-tests). In turn, the firing activity decreased when the mice were at the
252 onset of NREM sleep (Wake-to-NREM $P < 0.01$, , paired t-test), while on the other hand, the
253 transition from NREM to REM sleep was not marked by a substantial change in firing activity
254 (Fig 3I).

255

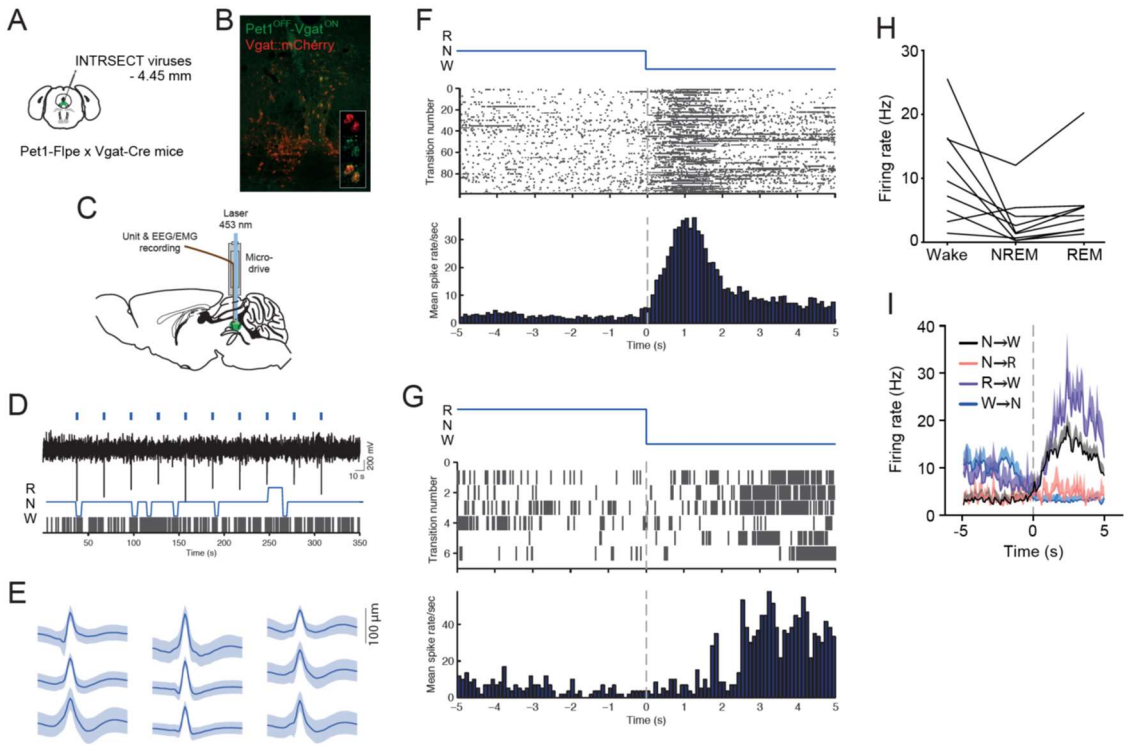

256

257 **Figure 3. The activity of optogenetically identified DR GABA neurons are modulated**
258 **across the sleep-wake cycle.** (A) Schematics of intersectional viral strategy: ChR2-Con/off-
259 eYFP was targeted to DR neurons in Pet1^{Flpe}-Vgat^{Cre} double transgenic mice. (B) ChR2
260 expression is restricted to DR GABA (Vgat-mCherry expressing) neurons. (C) Schematics of
261 the experimental design: simultaneous DR Pet1-OFF/Vgat-ON neuron and and EEG
262 recordings in behaving mice. (D) Example recording of a DRN Pet1-OFF/Vgat-ON neuron
263 throughout various sleep/wake states. (Top) raw trace voltage recording shows clear action
264 potential firing upon photostimulation (blue ticks). (Bottom) Hypnogram and spike ticks of the
265 neuron showed above (W: wake, R: REM, N: NREM). (E) Averaged spike waveforms of
266 optogenetically identified DRN Pet1-OFF/Vgat-ON neurons (n = 9 neurons from n = 4 mice).
267 DRN Pet1-OFF/Vgat-ON neurons were identified by their immediate firing in response to
268 pulses of blue light generated by a 453 nm laser (10 pulses of 5ms every 30 sec). (F,G) Raster
269 plot of a DRN Pet1-OFF/Vgat-ON neuron during NREM-to-wake transitions (F) and REM-to-

270 wake transitions (G) with spike ticks of the neuron (Top) and PSTH of the neuron across all
271 transitions (Bottom) (H) Firing rates of the 9 DRN Pet1-OFF/Vgat-ON neurons across
272 wakefulness, NREM and REM sleep. (I) PSTH (Mean + SEM) of DRN Pet1-OFF/Vgat-ON
273 neurons during the different sleep state transitions.

274

275 **Wake promoting effect of DR GABA neurons**

276 Next, we investigated whether Pet1-OFF/Vgat-ON neurons in the DR were causally involved
277 in arousal control. For this, we optogenetically activated DR Pet1-OFF/Vgat-ON neurons
278 during NREM sleep (see methods; Fig. 4C). Consistent with our correlative data, we found that
279 photostimulation of DR Pet1-OFF/Vgat-ON neurons induced a rapid arousal from NREM sleep
280 when light pulses were delivered at 20Hz as compared to controls ($P < 0.0001$, Three-way
281 ANOVA; Pet1-OFF/Vgat-ON vs Ctrl: $P < 0.0001$, Dunnett's multiple comparison's post-hoc
282 test), whereas 5Hz stimulation frequency did not decrease the latency to wakefulness transitions
283 (n = 6 animals per group; Fig 4C). The probability of REM sleep onset decreased upon
284 optogenetic activation of Pet1-OFF/Vgat-ON neurons during NREM sleep (Fig. 4E),
285 suggesting an implication in REM sleep onset. However, both 5 and 20Hz stimulation
286 frequencies during REM sleep led to an immediate arousal from REM sleep in Pet1-OFF/Vgat-
287 ON mice (Fig. 4D, $P < 0.0001$, three-way ANOVA; Pet1-OFF/Vgat-ON vs Ctrl: $P < 0.0001$, at
288 both 5 and 20 Hz, Dunnett's multiple comparison's post-hoc test). As expected, optogenetic
289 activation of Pet1-ON/Vgat-ON neurons (n = 6 animals) did not alter sleep-wake behavior as
290 compared to controls (n = 6 animals; Fig 4D, E).

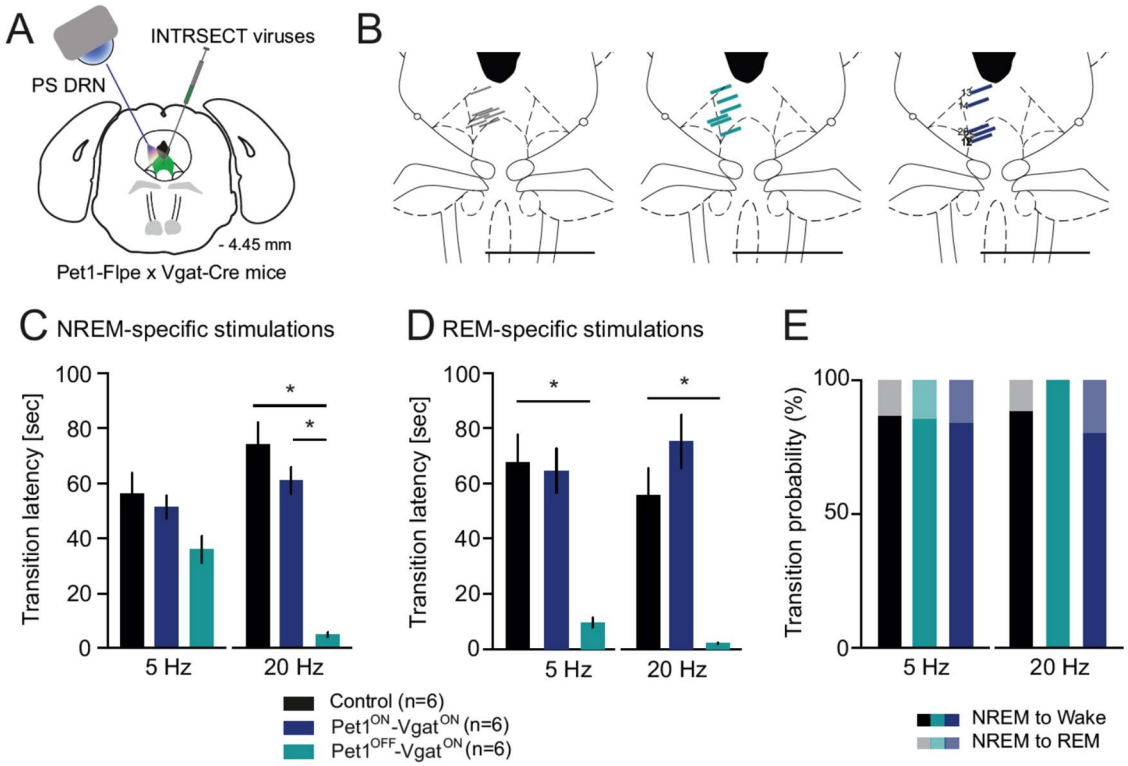

Figure 4. Stimulation of DRN GABAergic neurons promotes wakefulness. (A) Schematic of the experimental strategy: various intersectional viral constructs carrying the coding sequence of either eYFP (control) or ChR2 are injected in the DRN of Pet1^{Flpe} - Vgat^{Cre} double transgenic mice. The DRN is photostimulated 4 weeks post-infection. (B) Location of the fiberoptic canulae in all the animals used: left, gray lines: control, middle, green lines: Pet1-OFF/Vgat-ON, right, blue lines: Pet1-ON/Vgat-ON. (C) Latency of NREM to wake transition caused by the photostimulation of the DRN. (D) Latency of REM to wake transition caused by the photostimulation of the DRN. (E) State transition probabilities at 5 versus 20 Hz photostimulation for all three viral constructs. * $P < 0.05$.

DR GABA neurons promote Wake through disinhibition in LH

303 To identify potential sleep-wake centers that may mediate the arousal promotion of DR
304 GABAergic neurons, we performed a ChR2-assisted functional circuit mapping. Animals were
305 prepared as described above. We found that DR Pet1-OFF/Vgat-ON strongly innervated major
306 sleep-wake centers, such as the LH, the locus coeruleus (LC), the ventral tegmental area (VTA)
307 and the centromedial thalamic nucleus (CMT) (Fig. 5A and B). To further understand the
308 reciprocal connection between the DR and the LH, we performed optogenetic state-specific
309 stimulations of Pet1-OFF/Vgat-ON projecting fibers in the LH. We found that optogenetic
310 stimulation (20Hz) of DR Pet1-OFF/Vgat-ON projections to the LH reproduced the arousal-
311 inducing effect that was observed during somatic optogenetic activation (Fig. 5C, D, NREM
312 sleep: $P < 0.0001$, three-way ANOVA; Ctrl. versus LH stimulation: $P < 0.001$, Dunnett's
313 multiple comparisons post-hoc test; REM sleep: $P < 0.0001$, three-way ANOVA; Ctrl. versus
314 LH stimulation: $P < 0.001$, Dunnett's multiple comparisons post-hoc test). Interestingly,
315 optogentic activation of Pet1-OFF/Vgat-ON projections in the LC area, a predominant wake-
316 promoting center, resulted in a similar effect (Ctrl. versus LC stimulation: NREM sleep: $P<$
317 0.0001; REM sleep: $P < 0.001$, Dunnett's multiple comparisons post-hoc test), while
318 optogenetic stimulation of Pet1-OFF/Vgat-ON projections in the CMT led to an arousal only
319 from NREM sleep, but not from REM sleep (Ctrl. versus CMT stimulation: NREM sleep: $P<$
320 0.001; REM sleep: n.s., Dunnett's multiple comparisons post-hoc test), in line with a previous
321 study highlighting a role of the CMT in NREM sleep regulation (Gent et al., 2018) (Fig. 5 C,
322 D).

323

324 To further delineate the mechanism by which DR Pet1-OFF/Vgat-ON neurons induce arousal
325 via the LH, we performed single unit recordings in the LH while simultaneously recording
326 EEG/EMG and conducting optical stimulations of ChR2-expressing Pet1-OFF/Vgat-ON
327 neurons using a similar preparation as described above (see methods; Fig. 5E). First, we

clustered all the cells that we recorded in the LH according to their sleep-wake discharge profiles; recorded cells separated into 2 clusters, with one cluster showing maximal activity during wakefulness (55% of cells from 2 animals; Fig. 5F, G), while the second cluster showed maximal activity during both REM sleep and wakefulness (45% of cells from 2 animals; Fig. 55F, G). Cells from both clusters were less active during NREM sleep (Fig. 5F). Interestingly, during optogenetic stimulation of DR Pet1-OFF/Vgat-ON neurons, cells from Cluster 1 barely changed their firing rate, whereas half of the cells from the second cluster significantly modulated their firing activity in response to DR Pet1-OFF/Vgat-ON neuronal activation (Fig. 5G). In particular, a major part of responsive cells from Cluster 2 was disinhibited by the optogenetic activation of DR Pet1-OFF/Vgat ON neurons, while a few cells were inhibited (Fig. 5G and H, $P < 0.05$, three-way ANOVA). These results show that the activation of DR GABA neurons disinhibits the majority of LH neurons and promotes wakefulness.

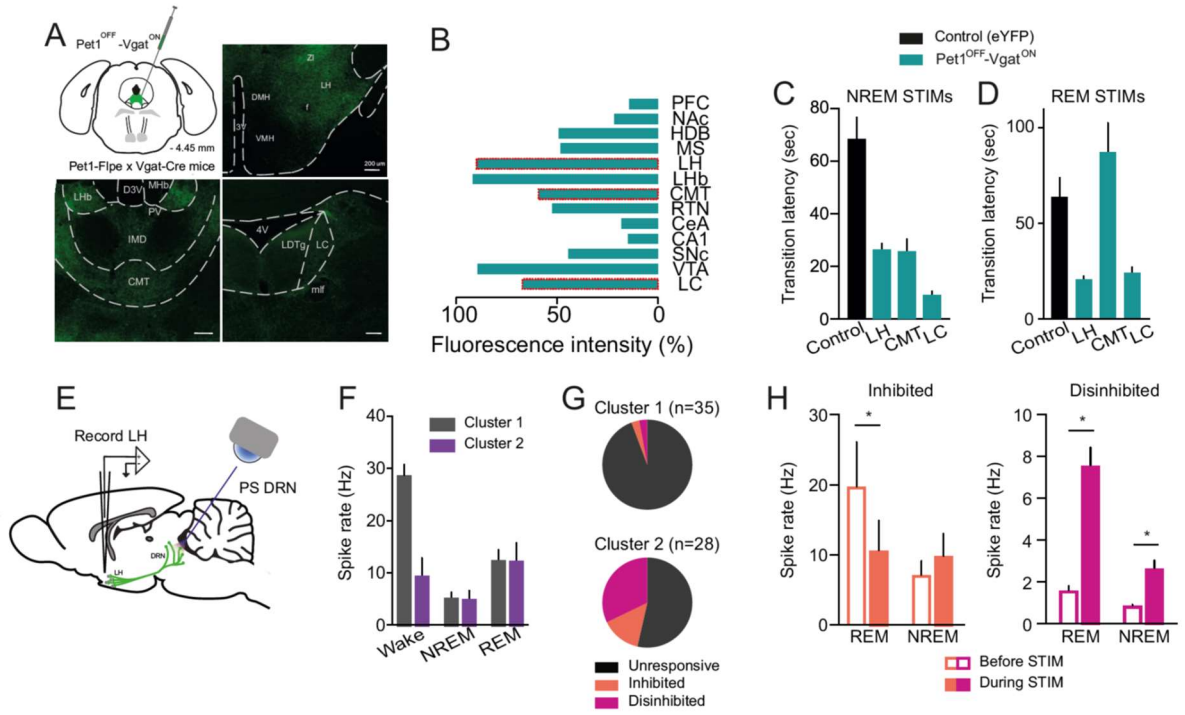

Figure 5. DRN GABA neurons promote arousal through disinhibition in the LH. (A) (Top left) Schematics of the experimental design: ChR2 is expressed in DRN GABAergic neurons

following a viral injection in Pet1-Flpe x Vgat-Cre mice. Axonal projections of DRN GABAergic neurons express ChR2 in various DRN target areas including the LH (top right), centromedial thalamus (CMT, bottom left) and locus coeruleus (LC, bottom right). (B) Normalized intensity of the fluorescent eYFP signal in various projection areas of the DRN (PFC: prefrontal cortex, NAc: nucleus accumbens, HDB: horizontal diagonal band of Brocca, MS: medial septum, LHb: lateral habenula, RTN: thalamic reticular nucleus, CeA: central amygdala, CA1: hippocampus CA1 region, SNc: substantia nigra pars compacta). (C) Latency of NREM to wake transition caused by photostimulation of DRN GABA projections in the LH, CMT and LC. (D) Latency of REM to wake transition caused by photostimulation of DRN GABA projection targets (LH, CMT, LC). (E) Schematic of the experimental design: ChR2 expressing Pet1-OFF/Vgat-ON neurons are photostimulated in the DRN while single units are recorded in the LH of freely moving mice. (F) Activity of all recorded LH neurons during various sleep-wake stages differentiates two clusters of neurons: Cluster 1 containing wake active neurons while Cluster 2 neurons do not show significant firing rate increases during the awake state. (G) Venn diagram of all Cluster 1 and 2 LH neurons constructed on the basis of their response to the photostimulation of DRN GABAergic neurons. (H) Effect of DRN GABAergic photostimulation on the state-dependent firing of inhibited (left) and disinhibited (right) neurons. For details see main text. * $P < 0.05$.

Discussion

In this study, we show that activation of LH GABAergic axons in the DR promotes wakefulness through a local release of GABA that rapidly and strongly suppresses activity of identified DR GABA neurons but disinhibits other non-GABAergic DR neurons. In addition, we found that the activity of DR GABA neurons is state dependent, while activation of DR GABA neurons disinhibits the majority of LH neurons to promote wakefulness. This wake promoting effect of

368 optogenetic activation of the LH GABA-DR GABA circuit promotes rapid wakefulness
369 selectively during NREM sleep, consistent with their activity profile across sleep-wake states
370 (Hassani et al., 2010; Herrera et al., 2016). These findings identify a LH GABA -DR GABA
371 feedback loop that is essential for rapid alteration of global brain states and facilitation of
372 wakefulness.

373

374 Using antero-and retrograde viral tracing and *in vitro* ChR_2 assisted circuit mapping we show
375 that a subset of LH GABA neurons establishes monosynaptic connections to DR neurons.
376 Functional analysis of this mapping revealed that LH GABA neurons exert a strong $GABA_A$-
377 mediated inhibitory action on DR GABAergic neurons leading to rapid NREM sleep-to-Wake
378 transitions. The precise neurochemical identity of this subset of DR-projecting LH GABA
379 neurons remains to be established in light of the numerous sub-populations amongst inhibitory
380 neurons of the LH (Mickelsen et al., 2017).

381

382 Local GABA release evoked by optogenetic activation of LH GABA axons in the DR promotes
383 wakefulness by rapidly and strongly suppressing the activity of DR GABA neurons. This occurs
384 through a direct synaptic inhibition of DR GABA neurons mediated by $GABA_A$ receptors and
385 leads to a prominent suppression of firing in DR GABA neurons *in vivo*. Consistent with
386 these *in vivo* recordings we show that the activity of identified DR GABA cells is strongly
387 modulated across NREM sleep-to-wake transitions and optogenetic activation of the LH
388 GABA-DR circuit promotes rapid wakefulness selectively during NREM sleep, but not during
389 REM sleep. This result is in line with previous studies reporting sleep/wake transitions upon
390 optogenetic activation of LH GABA fibers in the medial septum, locus coeruleus and reticular
391 thalamic nucleus (Herrera et al., 2016; Venner et al., 2016). Our results demonstrate that LH

392 GABA neurons directly inhibit DR GABA neurons that probably lead to a disinhibition of
393 various DR neurons. The exact targets of this disinhibition awaits further investigation and are
394 hard to predict given the extreme neurochemical and physiological diversity of the raphe nuclei
395 (Domonkos et al., 2016; Szonyi et al., 2016; Sos et al., 2017). A phasic increase in 5-HT neuron
396 activity can rapidly and prominently affect cortical activity (Lottem et al., 2016) and thus may
397 lead to brain state changes. However, recently the selective tonic activation of DR 5-HT neurons
398 has been shown to promote sleep, while burst stimulation induces wakefulness (Oikonomou et
399 al., 2019). In light of the present results, it is possible that the phasic activity changes of DR
400 neurons and their consequences at the cortical level at least partly originate from the LH GABA
401 neuron activation during sleep to wake transitions.

402

403 DR GABA neuronal stimulation also promoted wakefulness, possibly by suppressing or
404 activating local sleep- or wake-promoting neurons in the LH, respectively. One may speculate
405 that GABA release from DR GABA synapses could suppress activity of sleep-promoting
406 neurons including REM-sleep promoting MCH neurons (Jego et al., 2013; Konadhode et al.,
407 2013; Tsunematsu et al., 2014), REM active LH VGAT neurons (Hassani et al., 2010; Oesch
408 et al., 2020), REM-active Lh6x GABA neurons from the ventral zona incerta (Liu et al., 2017).
409 In contrast, it could inhibit local inhibitory circuits that would result in the activation of the
410 wake-promoting hypocretins/orexins neurons (Adamantidis et al., 2007), or wake-active LH
411 VGAT neurons (Hassani et al., 2010; Herrera et al., 2016; Oesch et al., 2020). Whether and
412 how this dual modulatory activity operates during the sleep-wake cycle awaits further
413 investigation.

414 Taken together, a brain area involved in energy balance and arousal can affect the activity of
415 the DR, an area involved in the control of higher brain functions including reward, patience,

416 mood and sensory coding suggesting a potential route for interactions between metabolic states
417 and brain states.
418

419 **MATERIALS AND METHODS**

420

421 All experimental procedures were performed according to the European Communities Council
422 Directives of 1986 (86/609/EEC) and 2003 (2003/65/CE) for animal research and were
423 approved by the Ethics Committee of the University of Szeged and University of Bern. 80 mice
424 were used in this study.

425

426 *Surgical procedures, viral injections*

427 Mice were anesthetized using 1-1.5% (v/v) Isoflurane, placed in a stereotaxic frame (Model
428 900, David Kopf Instruments, USA) on a heating pad (Supertech, Hungary). A small
429 craniotomy (1 mm diameter) was made over the LH (AP: -0.94; ML: ±1.00; DV: -5.2 and -5.4
430 (mm) from Bregma). 50 nl of undiluted virus (AAV-synapsin-ChR2-Venus(Petreanu et al.,
431 2009) in WT or GAD-GFP mice(Chattopadhyaya et al., 2004), AAV-flex-ChR2-RFP in
432 VGAT-cre mice) was injected in each hemisphere using a nanoinjector (Nanoliter 2000, WPI)
433 connected to a glass pipette (~20 um diameter). For the retrograde labeling of DR projecting
434 LH neurons, Ai9 mice (i.e. td tomato reporter mouse line(Madisen et al., 2010)) were injected
435 with PRV-cre (Oyibo et al., 2014) in the DR (AP: -4.75 , ML: 0, DV: -3.1 (mm) from Bregma;
436 31° AP angle). Mice received appropriate post operative care (analgesics: Rimadyl (15 mg/ml
437 (0,1 ml volume) i.p.), anti inflammatory drug: Dexafort (2mg/kg), antibiotic: Gentamicin
438 (5mg/kg).

439 **In vitro electrophysiology**

440 Mice were deeply anesthetized and perfused through the heart with ice cold cutting solution
441 containing (in mM) 93 *N*-methyl-d-glucamine, 2.5 KCl, 1.2 NaH_2PO_4, 30 $NaHCO_3$, 20 HEPES,
442 25 glucose, 5 *N*-acetyl-l-cysteine, 5 Na-ascorbate, 3 Na-pyruvate, 10 $MgSO_4$, and 0.5 $CaCl_2$.

443 The same solution was used to cut coronal brainstem slices containing the DR at 4ºC and for
444 the initial storage of slices (32-34ºC for 12 minutes) following which the slices were stored in
445 a solution containing (in mM) 30 NaCl, 2.5 KCl, 1.2 NaH_2PO_4, 1.3 $NaHCO_3$, 20 HEPES, 25
446 glucose, 5 *N*-acetyl-l-cysteine, 5 Na-ascorbate, 3 Na-pyruvate, 3 $CaCl_2$, and 1.5 $MgSO_4$. For
447 recording, slices were submerged in a chamber perfused with a warmed (34°C) continuously
448 oxygenated (95% O_2, 5% CO_2) ACSF containing (in mM) 130 NaCl, 3.5 KCl, 1 KH_2PO_4, 24
449 $NaHCO_3$, 1.5 $MgSO_4$, 3 $CaCl_2$, and 10 glucose. DR neurons were visualized using standard
450 DIC optics and recorded in whole cell current clamp mode using an EPC9 amplifier (Heka
451 Elektronik). Patch pipettes (tip resistance, 4–5 MΩ) were filled with an internal solution
452 containing the following (in mM): 126 K-gluconate, 4 KCl, 4 ATP-Mg, 0.3 GTP-Na_2, 10
453 HEPES, 10 kreatin-phosphate, and 8 biocytin, pH 7.25; osmolarity, 275 mOsm. The liquid
454 junction potential (−13 mV) was corrected off-line. Access and series resistances were
455 constantly monitored, and data from neurons with a >20% change from the initial value were
456 discarded. DR GABAergic neuron somata in GAD-GFP mice were targeted under
457 epifluorescent illumination. Photostimulation was performed through the microscope objective
458 using a blue LED light source (0.5-0.8 mW/mm^2, Thorlabs).
459

460 **In vivo electrophysiology**

461 To record the activity of DR neurons mice were anesthetized using 1-1.5% (v/v) Isoflurane
462 (Forane), placed in a stereotaxic frame (Model 900, David Kopf Instruments, USA) on a heating
463 pad (Supertech, Hungary). A small craniotomy (1 mm diameter) was made over the DR ((AP:
464 -4.75, ML: 0.0, DV: -3.1 (mm) from Bregma) leaving the dura mater intact. Glass electrodes
465 (resistance: 10-25 MOhm) were filled with saline containing 1.5% Biocytin (Sigma, Hungary).
466 The electrode was lowered in a 15º mediolateral angle to avoid the sagittal sinus. The activity
467 of DR neurons was monitored using a Multiclamp 700B amplifier (Molecular Devices)

468 operating in current clamp mode (filtered between 0.3 Hz and 3 kHz). At the end of some
469 recordings neurons were filled with Biocytin using 0.5-4 nA anodal current pulses of 500 ms
470 duration, 50% duty cycle for 2-10 minutes) as previously described (Pinault, 1996).

471

472 **Viral targeting**

473 For optogenetic activation of LH^{vgat} projections to the DR, one group of Vgat-IRES-Cre mice
474 (Vong et al., 2011) received AAV2-EF1a-DIO-hChR2(H134R)-eYFP, while the second group
475 received AAV2-EF1a-DIO-eYFP (control, both virus vectors were packaged at the Vector Core
476 of the University of North Carolina at Chapel Hill, titres between $3 \cdot 10^{12}$ to $5 \cdot 10^{12}$ cfu per ml).
477 For optogenetic activation of DR neurons, Vgat-IRES-Cre (Vong et al., 2011) x Pet1-Flpe
478 (Jensen et al., 2008) double transgenic mice received AAVdjd-EF1a-Foff/Con-
479 hChR2(H134R)-eYFP (Pet1-OFF/Vgat-ON), AAVdjd-EF1a-Fon/Con-hChR2(H134R)-eYFP
480 (Pet1-ON/Vgat-ON), or AAVdjd-EF1a-eYFP (eYFP controls). 0.6 ul of each virus was injected
481 bilaterally into the lateral hypothalamus (AP: -1.4 mm, ML: ±1 mm, DV: -5.4 mm from
482 Bregma) or into the dorsal raphe nucleus (AP: -4.45, ML: +1.2, DV: -2.9, at a 30° angle). The
483 virus suspension was infused with a micro-infusion pump (PHD Ultra, Harvard Apparatus)
484 through a 28 G stainless steel cannula (Plastic One) at a rate of 0.1 µl per minute.

485

486 **Surgical procedures for sleep experiments**

487 Surgical procedures for sleep-state-specific optogenetic experiments were performed as
488 described previously. Briefly, 8-10 week old male Vgat-IRES-Cre mice were chronically
489 implanted with an optical fibre (200 um, 0.39 NA Core Multimode Optical Fiber, FT200EMT,
490 TECS Clad, Thorlabs, inserted into zirconia ferrules, 1,25 mm OD; 230 µm ID, Precision Fiber
491 product) above the DR (AP -4.4, ML +1.2, DV -2.9 from Bregma), which were fixated to the

492 skull with C&B-Metabond (Parkell Inc.). Four stainless steel screw electrodes were inserted
493 epidurally (two into both frontal cortices, two into parietal cortices) for the recording of EEG
494 signals and wire loops were sewed to both neck muscles for EMG recordings. The EEG/EMG
495 electrodes and optic fibre were secured to the skull with dental cement (Patterson dental). After
496 surgical procedures mice were allowed to recover for two weeks.

497

498 **Data acquisition.**

499 Before the start of the experiment, the animals were habituated to a 3-m-long fibre optic patch
500 cord with protective tubing (Thorlabs) that was connected to the chronically implanted optical
501 fibre with a zirconia sleeve (Precision Fiber Products) and an EEG/EMG cable for one week.
502 Subsequently, a 24-h baseline polysomnographic recording was obtained without any
503 optogenetic manipulations. EEG and EMG signals were sampled with an AM systems 3500
504 amplifier at 512 Hz and digitized with a national instruments USB X DAQ device. EEG and
505 EMG data were recorded with the SleepScore software (View Point). All experiments took
506 place between 10 - 2 PM (Zeitgeber time 3-7).

507 For unit recordings in freely moving animals, mice were habituated to optical patch cords and
508 an electrode board head stage (RHD2132, Intan Technologies) for at least 4 days. Subsequently
509 a 24-h baseline polysomnographic recording was obtained without optogenetic manipulations
510 to ensure that the animals recovered a normal sleep-wake cycle. Tetrode signals were acquired
511 at 20 kHz with an open-source acquisition software (Open Ephys) via a digitizing head stage
512 (RHD2132) and a multi-channel DAQ board (Open Ephys, Intan Technologies). Opto-tagging
513 was performed by applying short blue light pulses to the DR (10 times 5ms pulses, every 30
514 seconds). Light-responsive cells were identified based on their spiking activity within 3 ms of
515 the application of blue light.

516

517

518 **EEG and EMG recordings**

519 Sleep-wake stages were scored based on EEG/EMG signal characteristics as described
520 previously (Jego *et al.*, 2013). Briefly, wakefulness was scored when low-amplitude
521 desynchronized EEG activity was accompanied by high, tonic muscle activity with phasic
522 bursts in the EMG. NREM sleep was defined by the presence of synchronized, high amplitude
523 oscillations in the delta frequency band (0.5 – 4 Hz) and low EMG tone. REM sleep was scored
524 when the EEG showed pronounced theta oscillations with an almost complete absence of EMG
525 tone except for short twitches. The 24 h baseline recordings were scored in epochs of 5 s, while
526 state-specific optogenetic stimulation recordings were scored at an epoch duration of 1 s.

527

528 **Optogenetic activation during polysomnographic recordings**

529 For *in vivo* optogenetic stimulation experiments, the patch cord was connected to a 473nm
530 DPSS laser (Laserglow Technologies) via a FC/PC connector (250 um, 30126G2-250,
531 Thorlabs). The laser output was set to a power output of 10 mW from the tip of the optic fibre.
532 Trains of 5 ms pulses at 5 or 20Hz were applied to LH_{VGAT} fibres or DR Pet1-OFF/Vgat-ON
533 neurons and fibres using a Master-9 pulse generator (A.M.P. Instruments). State-specific optical
534 activation was performed based on visual inspection of online EEG and EMG signal
535 parameters. For NREM and REM sleep-specific optogenetic activation, pulse trains were
536 applied through the patch cord and optic fibre when the animal spent at least 10 seconds in
537 NREM or REM sleep. The optogenetic stimulation was performed throughout the NREM or
538 REM episode until the mouse transitioned to another state. Afterwards, the animal was left
539 undisturbed to cycle between NREM sleep, REM sleep and wakefulness for 2-3 cycles before

540 the next NREM or REM sleep episode was optically stimulated. A total of 9 NREM and REM
541 sleep episodes per animal were optogenetically stimulated for each frequency (5 and 20 Hz).

542

543 **Immunohistochemistry following sleep studies**

544 At the end of the experiments, the mice were deeply anesthetized with an intraperitoneal
545 injection of pentobarbital (250 mg/kg, Streuli Pharma) and transcardially perfused with 5 ml
546 cold saline (0.9 % NaCl) followed by 20 ml 4% formaldehyde (Grogg Chemie). Subsequently,
547 the brains were removed and stored in formaldehyde over night at 4 °C for post-fixation. The
548 next day, the brains were transferred into phosphate-buffered saline (PBS) containing 30 %
549 sucrose before freezing. The brains were cut into 30 µm sections with a cryostat (Hyrax C 25,
550 Zeiss) and collected in PBS with 0.1 % Triton A-100 (Sigma-Aldrich), PBST.

551 For immunostaining, the sections were first incubated for 1 h at room temperature in a blocking
552 solution containing 4 % bovine serum albumin (Sigma-Aldrich) in PBS-T. Then the tissue was
553 incubated with anti-GFP (1:5000, A0262, Life technologies) and anti-Tph2 (1:400, ABN60,
554 Merck) for 24 h. Afterwards, the sections were washed for 5 x 5 minutes in PBS-T and then
555 incubated with DyLight 488 and AlexaFluor 555 secondary antibody (1:500 dilution, A96947
556 for eYFP, Life technologies; 1:500, A21428 for Tph2; Life technologies) at room temperature
557 for 1 h. The sections were washed 2 x 10 minutes in PBS-T and 2-10 minutes in PBS and then
558 mounted on glass slides. Cover slips were fixed on the slides with Fluoromount (F4680, Sigma-
559 Aldrich). Photomicrographs were taken using an Olympus BX 51 epifluorescence microscope.
560 For display, the image brightness and contrast was moderately adjusted in Adobe Photoshop
561 CC.

562

563 **Immunohistochemistry following *in vitro* recordings**

564 Following *in vivo* electrophysiological recordings, slices were immersed in 4%
565 paraformaldehyde (PFA) in 0.1 M phosphate buffer (PB; pH = 7.4) at 4 °C for at least 12 h.
566 After several washes with 0.1 M PB, slices were embedded in 10% gelatin, and further
567 sectioned into slices of 50-70 µm thickness in the cold PB using a vibratome VT1000S (Leica
568 Microsystems). Coronal sections were subjected to freeze-thaw over liquid nitrogen after
569 cryoprotecting in 10% and 20% sucrose. The recorded cells were first visualized with
570 incubation in Cy3-conjugated streptavidin (Jackson ImmunoResearch) for 2 h, diluted at 1:500
571 in tris buffer saline (TBS, SigmaAldrich). After examination by epifluorescence microscopy
572 (Olympus BX60), the sections containing the soma of the labeled neurons were incubated in
573 10% normal horse serumin (NHS) in TBS to block non specific antibody-binding sites. Free-
574 floating sections were incubated in primary antibodies dissolved in TBS containing 0,1%
575 Trinon X-100 ((TBS-Tx); Sigma Aldrich) for overnight at room temperature ((RT); 22 °C). The
576 following primary antibodies were used: anti-5HT-Rb (1:1000, Jackson ImmunoResearch);
577 anti-GABA-Rb (1:1000, Jackson ImmunoResearch). After several washes in TBS, the
578 immunoreactions were visualized with Dylight649-DARb (1:400, Jackson ImmunoResearch)
579 secondary antibodies. Finally, the sections were mounted in Vectashield mounting medium
580 (VectorLaboratories). Images were taken by confocal microscope (Olympus FV1000).

581

582 **Immunohistochemistry following *in vivo* single unit recordings**

583 After experiments the animal was quickly perfused through the heart with 50 ml of PBS
584 followed by 50 ml 4% PFA in 0.1 M PB. Following perfusion, brains were postfixed overnight
585 and stored in 0.1 M PB with 0.05% sodium azide at 4°C as a preservative. Tissue was sectioned
586 in PB at 50–70 µm on a Leica vibratome (Leica VT 1000S). Coronal sections were
587 permeabilized in 0.3 % TBS-Tx. The sections were incubated in Cy3 or Alexa488 conjugated

588 streptavidin (1:500; Jackson ImmunoResearch) for 2 h at RT in TBS. Images were taken by
589 confocal microscope (Olympus FV1000).

590

591 **Permutation test for significant modulation of unit spiking during photostimulation**

592 The firing rate change of single units upon photostimulation was assessed by subtracting the
593 average spike rate during the 10 seconds preceding the stimulation from the average spike rate
594 during optogenetic activation. To test for significant modulation, 9999 stimulation onsets were
595 randomly drawn from each single unit's activity time series and the firing rate change across
596 these random onsets was calculated. If the actual firing rate difference was larger than 95% or
597 smaller than 5% of the randomly calculated ones, the firing of the neuron was significantly
598 modulated during this photostimulation. Inhibited or disinhibited neurons showed a significant
599 decrease or increase, respectively, of their firing rate during more than 50% of all
600 photostimulations. Neurons whose firing rate was significantly modulated during less than 50%
601 of all optogenetic stimulations are reported as unresponsive.

602

603 **Data analysis**

604 Data analysis was performed using Spike2: (Cambridge Electronic Design, England),
605 OriginPro 8.5 (MicroCal, USA), IgorPro (WaveMetrics, USA), Matlab (MathWorks, USA) and
606 Prism (GraphPad, USA) software. The data were tested for normality with the Shapiro-Wilk
607 and the Kolmogorov-Smirnov tests and accordingly analysed using parametric or non-
608 parametric methods. We used three-way ANOVA to test for frequency (5 versus 20 Hz, within-
609 group comparisons) and opsin (eYFP controls versus ChR2-expressing mice, between-groups
610 comparisons) effects in the latencies to transition to another state from NREM or REM sleep
611 of state-specific optogenetic activation experiments. PSPs evoked by photostimulation were

detected in Vm recordings using a threshold of 2xSD in a ± 50 ms time window following photostimulation. Action potentials in extracellular recordings were detected in Spike2 using a straight forward level threshold. Firing rate histograms were computed for each photostimulation trial of each neuron. The control period was defined as 0.5 seconds before photostimulation. All data are displayed as averages +/- s.e.m.

Acknowledgements

This work has been supported by the Hungarian Scientific Research Fund (grant NF 123831 to M.L.L.), the Hungarian Brain Research Program (grant KTIA_NAP_13-2-2014-0014 to M.L.L.), NIH R01 DA034022 (S.M.D.) and the German Research Foundation (GA 2410/1-1 to M.G.).

625

626 REFERENCES

627 Adamantidis AR, Zhang F, Aravanis AM, Deisseroth K, de Lecea L (2007) Neural substrates
628 of awakening probed with optogenetic control of hypocretin neurons. Nature 450:420-
629 424.

630 Allers KA, Sharp T (2003) Neurochemical and anatomical identification of fast- and slow-firing
631 neurones in the rat dorsal raphe nucleus using juxtacellular labelling methods in vivo.
632 Neuroscience 122:193-204.

633 Bang SJ, Commons KG (2012) Forebrain GABAergic projections from the dorsal raphe
634 nucleus identified by using GAD67-GFP knock-in mice. The Journal of comparative
635 neurology 520:4157-4167.

636 Bernardis LL, Bellinger LL (1996) The lateral hypothalamic area revisited: ingestive behavior.
637 Neuroscience and biobehavioral reviews 20:189-287.

638 Bonnavion P, Mickelsen LE, Fujita A, de Lecea L, Jackson AC (2016) Hubs and spokes of the
639 lateral hypothalamus: cell types, circuits and behaviour. The Journal of physiology
640 594:6443-6462.

641 Carter ME, Adamantidis A, Ohtsu H, Deisseroth K, de Lecea L (2009) Sleep homeostasis
642 modulates hypocretin-mediated sleep-to-wake transitions. The Journal of neuroscience
643 : the official journal of the Society for Neuroscience 29:10939-10949.

644 Carter ME, Yizhar O, Chikahisa S, Nguyen H, Adamantidis A, Nishino S, Deisseroth K, de
645 Lecea L (2010) Tuning arousal with optogenetic modulation of locus coeruleus neurons.
646 Nature neuroscience 13:1526-1533.

647 Cespuglio R, Walker E, Gomez ME, Musolino R (1976) Cooling of the nucleus raphe dorsalis
648 induces sleep in the cat. Neuroscience letters 3:221-227.

649 Chattopadhyaya B, Di Cristo G, Higashiyama H, Knott GW, Kuhlman SJ, Welker E, Huang ZJ
650 (2004) Experience and activity-dependent maturation of perisomatic GABAergic
651 innervation in primary visual cortex during a postnatal critical period. The Journal of
652 neuroscience : the official journal of the Society for Neuroscience 24:9598-9611.
653 Cohen JY, Amoroso MW, Uchida N (2015) Serotonergic neurons signal reward and
654 punishment on multiple timescales. eLife 4.
655 Constantinople CM, Bruno RM (2011) Effects and mechanisms of wakefulness on local cortical
656 networks. Neuron 69:1061-1068.
657 Correia PA, Lottem E, Banerjee D, Machado AS, Carey MR, Mainen ZF (2017) Transient
658 inhibition and long-term facilitation of locomotion by phasic optogenetic activation of
659 serotonin neurons. eLife 6.
660 Descarries L, Watkins KC, Garcia S, Beaudet A (1982) The serotonin neurons in nucleus raphe
661 dorsalis of adult rat: a light and electron microscope radioautographic study. The Journal
662 of comparative neurology 207:239-254.
663 Domonkos A, Nikitidou Ledri L, Laszlovszky T, Cserep C, Borhegyi Z, Papp E, Nyiri G,
664 Freund TF, Varga V (2016) Divergent in vivo activity of non-serotonergic and
665 serotonergic VGluT3-neurones in the median raphe region. The Journal of physiology
666 594:3775-3790.
667 Dugovic C, Wauquier A (1987) 5-HT2 receptors could be primarily involved in the regulation
668 of slow-wave sleep in the rat. European journal of pharmacology 137:145-146.
669 Eggermann E, Kremer Y, Crochet S, Petersen CCH (2014) Cholinergic signals in mouse barrel
670 cortex during active whisker sensing. Cell reports 9:1654-1660.
671 Fenno LE, Mattis J, Ramakrishnan C, Hyun M, Lee SY, He M, Tucciarone J, Selimbeyoglu A,
672 Berndt A, Grosenick L, Zalocusky KA, Bernstein H, Swanson H, Perry C, Diester I,

673 Boyce FM, Bass CE, Neve R, Huang ZJ, Deisseroth K (2014) Targeting cells with single
674 vectors using multiple-feature Boolean logic. Nature methods 11:763-772.
675 Fiske EP, C.M.; Grønli, J.; Sørensen, E.; Bjorvatn, B.; Bjørkum, A.A.; Ursin, R. (2008)
676 Increased extracellular 5-HT but no change in sleep after perfusion of a 5-HT1A
677 antagonist into the dorsal raphe nucleus of rats. Acta Physiol (Oxf) 193:89-97.
678 Fonseca MS, Murakami M, Mainen ZF (2015) Activation of dorsal raphe serotonergic neurons
679 promotes waiting but is not reinforcing. Current biology : CB 25:306-315.
680 Gent TC, Bandarabadi M, Herrera CG, Adamantidis AR (2018) Thalamic dual control of sleep
681 and wakefulness. Nature neuroscience 21:974-984.
682 Hassani OK, Henny P, Lee MG, Jones BE (2010) GABAergic neurons intermingled with orexin
683 and MCH neurons in the lateral hypothalamus discharge maximally during sleep. The
684 European journal of neuroscience 32:448-457.
685 Herrera CG, Cadavieco MC, Jego S, Ponomarenko A, Korotkova T, Adamantidis A (2016)
686 Hypothalamic feedforward inhibition of thalamocortical network controls arousal and
687 consciousness. Nature neuroscience 19:290-298.
688 Huang KW, Ochandarena NE, Philson AC, Hyun M, Birnbaum JE, Cicconet M, Sabatini BL
689 (2019) Molecular and anatomical organization of the dorsal raphe nucleus. eLife 8.
690 Idzikowski C, Mills FJ, Glennard R (1986) 5-Hydroxytryptamine-2 antagonist increases human
691 slow wave sleep. Brain research 378:164-168.
692 Ito H, Yanase M, Yamashita A, Kitabatake C, Hamada A, Suhara Y, Narita M, Ikegami D,
693 Sakai H, Yamazaki M, Narita M (2013) Analysis of sleep disorders under pain using an
694 optogenetic tool: possible involvement of the activation of dorsal raphe nucleus-
695 serotonergic neurons. Molecular brain 6:59.

696 Iwasaki K, Komiya H, Kakizaki M, Miyoshi C, Abe M, Sakimura K, Funato H, Yanagisawa M
697 (2018) Ablation of Central Serotonergic Neurons Decreased REM Sleep and Attenuated
698 Arousal Response. Frontiers in neuroscience 12:535.
699 Jego S, Glasgow SD, Herrera CG, Ekstrand M, Reed SJ, Boyce R, Friedman J, Burdakov D,
700 Adamantidis AR (2013) Optogenetic identification of a rapid eye movement sleep
701 modulatory circuit in the hypothalamus. Nature neuroscience 16:1637-1643.
702 Jensen P, Farago AF, Awatramani RB, Scott MM, Deneris ES, Dymecki SM (2008) Redefining
703 the serotonergic system by genetic lineage. Nature neuroscience 11:417-419.
704 Jones BE (2020) Arousal and sleep circuits. Neuropsychopharmacology : official publication
705 of the American College of Neuropsychopharmacology 45:6-20.
706 Jouvet M (1968) Insomnia and decrease of cerebral 5-hydroxytryptamine after destruction of
707 the raphe system in the cat. Advances in pharmacology 6:265-279.
708 Jouvet M (1972) The role of monoamines and acetylcholine-containing neurons in the
709 regulation of the sleep-waking cycle. Ergebnisse der Physiologie, biologischen Chemie
710 und experimentellen Pharmakologie 64:166-307.
711 Kapoor V, Provost AC, Agarwal P, Murthy VN (2016) Activation of raphe nuclei triggers rapid
712 and distinct effects on parallel olfactory bulb output channels. Nature neuroscience
713 19:271-282.
714 Koella WP (1968) Discussion of insomnia and decrease of cerebral 5-hydroxytryptamine after
715 destruction of the raphe system in the cat. Advances in pharmacology 6:280-282.
716 Konadhode RR, Pelluru D, Blanco-Centurion C, Zayachkivsky A, Liu M, Uhde T, Glen WB,
717 Jr., van den Pol AN, Mulholland PJ, Shiromani PJ (2013) Optogenetic stimulation of
718 MCH neurons increases sleep. The Journal of neuroscience : the official journal of the
719 Society for Neuroscience 33:10257-10263.

720 Liu K, Kim J, Kim DW, Zhang YS, Bao H, Denaxa M, Lim SA, Kim E, Liu C, Wickersham
721 IR, Pachnis V, Hattar S, Song J, Brown SP, Blackshaw S (2017) Lhx6-positive GABA-
722 releasing neurons of the zona incerta promote sleep. Nature 548:582-587.
723 Liu Z, Zhou J, Li Y, Hu F, Lu Y, Ma M, Feng Q, Zhang JE, Wang D, Zeng J, Bao J, Kim JY,
724 Chen ZF, El Mestikawy S, Luo M (2014) Dorsal raphe neurons signal reward through
725 5-HT and glutamate. Neuron 81:1360-1374.
726 Lottem E, Lorincz ML, Mainen ZF (2016) Optogenetic Activation of Dorsal Raphe Serotonin
727 Neurons Rapidly Inhibits Spontaneous But Not Odor-Evoked Activity in Olfactory
728 Cortex. The Journal of neuroscience : the official journal of the Society for
729 Neuroscience 36:7-18.
730 Lowry CA, Hale MW, Evans AK, Heerkens J, Staub DR, Gasser PJ, Shekhar A (2008)
731 Serotonergic systems, anxiety, and affective disorder: focus on the dorsomedial part of
732 the dorsal raphe nucleus. Annals of the New York Academy of Sciences 1148:86-94.
733 Madisen L, Zwingman TA, Sunkin SM, Oh SW, Zariwala HA, Gu H, Ng LL, Palmiter RD,
734 Hawrylycz MJ, Jones AR, Lein ES, Zeng H (2010) A robust and high-throughput Cre
735 reporting and characterization system for the whole mouse brain. Nature neuroscience
736 13:133-140.
737 McGinty DJ, Harper RM (1976) Dorsal raphe neurons: depression of firing during sleep in cats.
738 Brain research 101:569-575.
739 Mickelsen LE, Kolling FWt, Chimileski BR, Fujita A, Norris C, Chen K, Nelson CE, Jackson
740 AC (2017) Neurochemical Heterogeneity Among Lateral Hypothalamic
741 Hypocretin/Orexin and Melanin-Concentrating Hormone Neurons Identified Through
742 Single-Cell Gene Expression Analysis. eNeuro 4.

743 Miyazaki K, Miyazaki KW, Doya K (2011) Activation of dorsal raphe serotonin neurons
744 underlies waiting for delayed rewards. The Journal of neuroscience : the official journal
745 of the Society for Neuroscience 31:469-479.
746 Monti JM (2011) Serotonin control of sleep-wake behavior. Sleep medicine reviews 15:269-
747 281.
748 Mouret J, Vilppula A, Frachon N, Jouvet M (1968) [Effects of a monoanime oxidase inhibitor
749 on sleep in rats]. Comptes rendus des seances de la Societe de biologie et de ses filiales
750 162:914-917.
751 Oesch LT, Gazea M, Gent TC, Bandarabadi M, Gutierrez Herrera C, Adamantidis AR (2020)
752 REM sleep stabilizes hypothalamic representation of feeding behavior. Proceedings of
753 the National Academy of Sciences of the United States of America 117:19590-19598.
754 Oikonomou G, Altermatt M, Zhang RW, Coughlin GM, Montz C, Gradinaru V, Prober DA
755 (2019) The Serotonergic Raphe Promote Sleep in Zebrafish and Mice. Neuron 103:686-
756 701 e688.
757 Okaty BW, Sturrock N, Escobedo Lozoya Y, Chang Y, Senft RA, Lyon KA, Alekseyenko OV,
758 Dymecki SM (2020) A single-cell transcriptomic and anatomic atlas of mouse dorsal
759 raphe Pet1 neurons. eLife 9.
760 Oyibo HK, Znamenskiy P, Oviedo HV, Enquist LW, Zador AM (2014) Long-term Cre-
761 mediated retrograde tagging of neurons using a novel recombinant pseudorabies virus.
762 Frontiers in neuroanatomy 8:86.
763 Petreanu L, Mao T, Sternson SM, Svoboda K (2009) The subcellular organization of neocortical
764 excitatory connections. Nature 457:1142-1145.
765 Pinault D (1996) A novel single-cell staining procedure performed in vivo under
766 electrophysiological control: morpho-functional features of juxtacellularly labeled

767 thalamic cells and other central neurons with biocytin or Neurobiotin. Journal of
768 neuroscience methods 65:113-136.
769 Popa D, Lena C, Fabre V, Prenat C, Gingrich J, Escourrou P, Hamon M, Adrien J (2005)
770 Contribution of 5-HT2 receptor subtypes to sleep-wakefulness and respiratory control,
771 and functional adaptations in knock-out mice lacking 5-HT2A receptors. The Journal of
772 neuroscience : the official journal of the Society for Neuroscience 25:11231-11238.
773 Portas CM, Bjorvatn B, Ursin R (2000) Serotonin and the sleep/wake cycle: special emphasis
774 on microdialysis studies. Progress in neurobiology 60:13-35.
775 Pytliak M, Vargova V, Mechirova V, Felsoci M (2011) Serotonin receptors - from molecular
776 biology to clinical applications. Physiological research 60:15-25.
777 Reimer J, McGinley MJ, Liu Y, Rodenkirch C, Wang Q, McCormick DA, Tolias AS (2016)
778 Pupil fluctuations track rapid changes in adrenergic and cholinergic activity in cortex.
779 Nature communications 7:13289.
780 Ren J, Isakova A, Friedmann D, Zeng J, Grutzner SM, Pun A, Zhao GQ, Kolluru SS, Wang R,
781 Lin R, Li P, Li A, Raymond JL, Luo Q, Luo M, Quake SR, Luo L (2019) Single-cell
782 transcriptomes and whole-brain projections of serotonin neurons in the mouse dorsal
783 and median raphe nuclei. eLife 8.
784 Sakai K (2011) Sleep-waking discharge profiles of dorsal raphe nucleus neurons in mice.
785 Neuroscience 197:200-224.
786 Saper CB, Chou TC, Scammell TE (2001) The sleep switch: hypothalamic control of sleep and
787 wakefulness. Trends in neurosciences 24:726-731.
788 Saper CB, Fuller PM, Pedersen NP, Lu J, Scammell TE (2010) Sleep state switching. Neuron
789 68:1023-1042.

790 Seo C, Guru A, Jin M, Ito B, Sleezer BJ, Ho YY, Wang E, Boada C, Krupa NA, Kullakanda
791 DS, Shen CX, Warden MR (2019) Intense threat switches dorsal raphe serotonin
792 neurons to a paradoxical operational mode. Science 363:538-542.
793 Smith HR, Leibold NK, Rappoport DA, Ginapp CM, Purnell BS, Bode NM, Alberico SL, Kim
794 YC, Audero E, Gross CT, Buchanan GF (2018) Dorsal Raphe Serotonin Neurons
795 Mediate CO2-Induced Arousal from Sleep. The Journal of neuroscience : the official
796 journal of the Society for Neuroscience 38:1915-1925.
797 Solarewicz JZ, Angoa-Perez M, Kuhn DM, Mateika JH (2015) The sleep-wake cycle and motor
798 activity, but not temperature, are disrupted over the light-dark cycle in mice genetically
799 depleted of serotonin. American journal of physiology Regulatory, integrative and
800 comparative physiology 308:R10-17.
801 Sommerfelt L, Ursin R (1993) The 5-HT2 antagonist ritanserin decreases sleep in cats. Sleep
802 16:15-22.
803 Sos KE, Mayer MI, Cserep C, Takacs FS, Szonyi A, Freund TF, Nyiri G (2017) Cellular
804 architecture and transmitter phenotypes of neurons of the mouse median raphe region.
805 Brain structure & function 222:287-299.
806 Szonyi A, Mayer MI, Cserep C, Takacs VT, Watanabe M, Freund TF, Nyiri G (2016) The
807 ascending median raphe projections are mainly glutamatergic in the mouse forebrain.
808 Brain structure & function 221:735-751.
809 Torda C (1967) Effect of brain serotonin depletion on sleep in rats. Brain research 6:375-377.
810 Trulson ME, Jacobs BL (1979) Raphe unit activity in freely moving cats: correlation with level
811 of behavioral arousal. Brain research 163:135-150.
812 Tsunematsu T, Ueno T, Tabuchi S, Inutsuka A, Tanaka KF, Hasuwa H, Kilduff TS, Terao A,
813 Yamanaka A (2014) Optogenetic manipulation of activity and temporally controlled
814 cell-specific ablation reveal a role for MCH neurons in sleep/wake regulation. The

815 Journal of neuroscience : the official journal of the Society for Neuroscience 34:6896-
816 6909.
817 Urbain N, Creamer K, Debonnel G (2006) Electrophysiological diversity of the dorsal raphe
818 cells across the sleep-wake cycle of the rat. The Journal of physiology 573:679-695.
819 Venner A, Anaclet C, Broadhurst RY, Saper CB, Fuller PM (2016) A Novel Population of
820 Wake-Promoting GABAergic Neurons in the Ventral Lateral Hypothalamus. Current
821 biology : CB 26:2137-2143.
822 Vong L, Ye C, Yang Z, Choi B, Chua S, Jr., Lowell BB (2011) Leptin action on GABAergic
823 neurons prevents obesity and reduces inhibitory tone to POMC neurons. Neuron
824 71:142-154.
825 Weber F, Dan Y (2016) Circuit-based interrogation of sleep control. Nature 538:51-59.
826 Whitney MS, Shemery AM, Yaw AM, Donovan LJ, Glass JD, Deneris ES (2016) Adult Brain
827 Serotonin Deficiency Causes Hyperactivity, Circadian Disruption, and Elimination of
828 Siestas. The Journal of neuroscience : the official journal of the Society for
829 Neuroscience 36:9828-9842.

830

831